Geometry and torsional motion of biphenyl in the ground and first excited singlet state

Hoong-Sun Im and E. R. Bernstein

Citation: The Journal of Chemical Physics **88**, 7337 (1988); doi: 10.1063/1.454345

Geometry and torsional motion of biphenyl in the ground and first excited singlet state

Hoong-Sun Im and E. R. Bernstein
Department of Chemistry, Colorado State University, Fort Collins, Colorado 80523

(Received 13 January 1988; accepted 2 March 1988)

The lowest excited singlet state of biphenyl (BP) and a number of its isotopically and chemically substituted analogs have been studied by supersonic jet laser spectroscopy. The symmetry species of this excited state in BP can be classified as B_{2u}^+ in the G_{16} extended molecular symmetry group G_{16} (EM). The symmetry-allowed origin of the biphenyl -h_{10} $S_1 \leftarrow S_0$ electronic transition occurs at 35 268 cm^{-1}. The frequency of the torsional motion in S_1 is determined to be ~ 65 cm^{-1}. The potential parameters for this motion in S_1 are $V_2 = 1195$ cm^{-1}, $V_4 = -190$ cm^{-1}, and $V_6 = 18$ cm^{-1}. The torsional motion for the ground state (~ 50 cm^{-1}) can be described by $V_2 = 50$ cm^{-1} and $V_4 = -148$ cm^{-1}. The change in the dihedral angle between the two benzene rings in BP upon S_0 to S_1 excitation is determined to be $\sim 44°$ based on a Franck–Condon factor calculation. Several fundamentals of the molecular vibrations are assigned in the S_1 state. The exciton interaction between the coupled benzene rings in biphenyl is suggested to be large ($> 10^3$ cm^{-1}).

I. INTRODUCTION

Biaryl molecules, of which biphenyl is the prototypic example, are of fundamental interest for two reasons. First, they are typically composed of two chromophores coupled by a single C–C bond so their energy levels and dynamical behavior can be thought of in terms of these two interacting moieties. In fact, exciton or exchange interaction between the two halves of the molecules has often been invoked to explain the electronic properties of biaryl molecules.[1] Second, the conformational structure and dynamics of these molecules give insight into the behavior of nonrigid large molecules. These important concerns notwithstanding, a detailed study of the vibronic states of biaryl molecules in general, and biphenyl in particular, is difficult due to the diffuseness of their gas phase spectra. The broad featureless gas phase absorption spectra of these systems are due to hot band transitions from low lying (torsional) vibrations of the ground state. Condensed phase spectra, on the other hand, cannot be used to determine structure, interactions, and dynamics of these nonrigid molecules because these properties are greatly perturbed by the condensed phase intermolecular interactions.

Expansion of biaryl molecules in a supersonic jet circumvents these problems: hot bands are removed from the spectrum and structural data derived from an analysis of the spectroscopic data pertain to the free molecule. Supersonic molecular jet laser spectroscopy has been employed in the past to study various biaryl systems. Low frequency modes and torsional potentials have been identified through laser jet spectroscopy in 1,1′-binaphthyl,[2] 9-phenyl-anthracene and its derivatives,[3] and 9,9′-bianthryl.[4]

Biphenyl, on the other hand, has proven difficult to study even with jet cooling techniques. A complete analysis of the biphenyl molecular absorption spectrum is not available, although the torsional frequency in the excited state has been assigned.[5] Biphenyl undergoes a large conformational change upon excitation ($S_1 \leftarrow S_0$)[6] and the inter-ring exciton interaction is quite large for the planar excited state.[7] Consequently experimental and theoretical perturbation approaches to analysis of the biphenyl spectrum have not been terribly fruitful.

Since biphenyl is a nonrigid molecule which undergoes a large geometry change upon excitation from S_0 to S_1, point groups are not appropriate for the determination of spectroscopic selection rules. In such circumstances, molecular symmetry groups developed by Longuet-Higgins, Bunker, and others[8] must be generated and employed. We develop and employ in this work the appropriate extended molecular symmetry group[8(d)] for biphenyl [G_{16} (EM)] and classify the electronic, torsional, and vibrational states according to its irreducible representation.

In this paper we report supersonic molecular jet mass selected excitation spectra for biphenyl and a number of its isotopic and chemical derivatives. The proper selection rules are obtained for the vibronic–contorsional transitions of this molecule based on the G_{16} extended molecular symmetry group G_{16} (EM). Based on these data and considerations, the origin for the biphenyl $S_1 \leftarrow S_0$ transition is suggested and the spectrum is analyzed in detail up to 900 cm^{-1} from this origin. Potential parameters for the torsional motion in both S_0 and S_1 are presented. The conformational change between S_0 and S_1 is determined by simulating the intensity pattern found in the torsional progression. This calculation is carried out employing the eigenvectors of the torsional modes. Finally, data obtained from the spectra of isotopic and chemically substituted biphenyls are used to determine the exciton interaction between the two rings in the excited state.

II. EXPERIMENTAL PROCEDURES

The experimental apparatus has been described in detail previously.[9] A pulsed valve is used to generate the molecular beam. Samples are placed inside the valve and heated near their melting points to increase their concentration in the beam. The supersonic molecular beam passes through a

0021-9606/88/127337-11$02.10

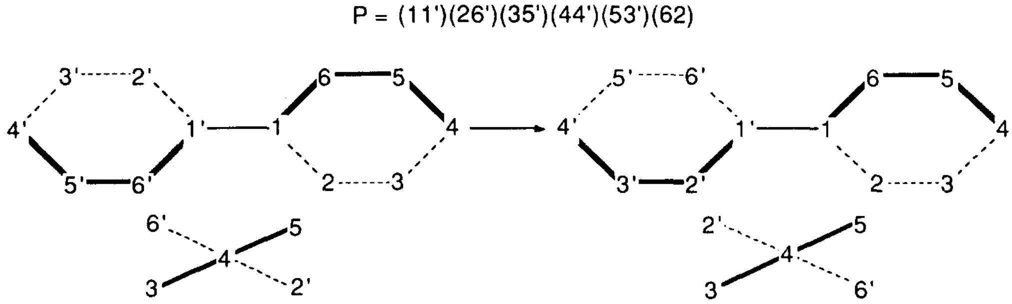

FIG. 1. A feasible conformational transformation in G_{16} (EM), which is not possible in the D_{2h} symmetry point group. The symmetry element for this transformation is given in the figure. The transformation is a rotation of one benzene ring by 180° about the inter-ring C–C single bond. The atom numbering of BP-h_{10} is also shown.

skimmer and then into the ionization region of a time-of-flight mass spectrometer (TOFMS). The cold molecules are excited to S_1 by the doubled output of a Nd^{+3}/YAG pumped pulsed dye laser focused into the ionization region. The light intersects the molecular beam at right angles to its direction of travel. The flight tube is perpendicular to these two directions. A second photon of this beam is absorbed to create the ion (e.g., $\mathrm{C_{12}H_{10}^{+}}$).

Biphenyl-h_{10} (BP-h_{10}), 4-methylbiphenyl (4-$\mathrm{CH_3}$–BP), 4,4'-dimethylbiphenyl [4,4'-$\mathrm{(CH_3)_2}$–BP], and 4,4'-difluorobiphenyl [4,4'-$\mathrm{(F)_2}$–BP] are obtained from Aldrich. The biphenyl-d_{10} (BP-d_{10}) is purchased from MSD Isotopes. Samples of 4-fluorobiphenyl (4-F–BP), 2-fluorobiphenyl (2-F–BP), and 4-chlorobiphenyl (4-Cl–BP) are purchased from Pfaltz and Bauer. The samples of 4-deutromethylbiphenyl (4-$\mathrm{CD_3}$–BP) and half deuterated biphenyl (BP-h_5d_5) are provided by J. I. Seeman and H. V. Secor who synthesized them at Philip Morris USA Research Center. All samples are studied as received and not further purified.

Biphenyl and many of its derivatives do not readily cool in a supersonic expansion. Several carrier gases are used to cool these molecules: high pressure He (~10 atm), He/$\mathrm{CF_4}$ mixtures, He/Ar mixtures, $\mathrm{N_2}$ and Ar. Pure Ar (~2–3 atm) is apparently the best expansion gas in terms of cooling BP and its derivatives. BP/Ar clusters, which undoubtedly form in this expansion, do not interfere with these studies because mass detection is employed in all experiments and the reported features appear in all expansion gases employed.

III. GROUP THEORETICAL CONSIDERATIONS

A. Molecular symmetry group for biphenyl

The ground state equilibrium geometry of biphenyl is not planar: the dihedral angle between the two rings is $42 \pm 2°$.[10] The excited geometry is planar[6] (*vida infra*). The point group for the ground state molecule is D_2 and the point group for the excited state molecule is D_{2h}. Neither point group is of course adequate for a treatment of the vibronic transitions of BP. Further, if torsional tunneling is feasible in either state, the BP molecule must be considered nonrigid. Various conformers of BP are possible if the molecule is nonrigid; e.g., see Fig. 1. Thus, point groups are inadequate in describing the behavior of the nonrigid, spectroscopically accessed BP molecule.

Molecular symmetry groups,[8] composed of permutation and permutation–inversion elements, are employed for the study of nonrigid molecules in general. Following the procedure outlined by Bunker,[8(d)] the appropriate molecular symmetry group can be established for BP: the group is G_{16} (MS). BP is, however, a molecule composed of equivalent rotors joined by a single bond in a linear fashion (similar to dimethylacetylene) and thereby admits a double valuedness for the torsional coordinate. Two coordinate transformations correspond to each element of G_{16} (MS). The G_{16} (MS) group must be extended (like the "spin–double" groups are for point groups) to generate the extended molecular symmetry group G_{16} (EM).[8(d)]

The permutation–inversion groups isomorphic to D_2 and D_{2h} point groups are subgroups of G_{16} (EM). The correlation between G_{16} (EM) and these subgroups is given in Table I.

B. Symmetry species in G_{16} (EM)

1. Dipole moments

The molecule fixed x, y, z axes are chosen such that z is the longest axis containing the inter-ring single bond, x bisects the smaller inter-ring dihedral angle α of the equilibrium geometry in the ground state, and y is perpendicular to

TABLE I. The correlation table of G_{16} (EM) with D_2 and D_{2h} symmetry group.

G_{16} (EM)[a]	D_{2h}	D_2
A_{1g}^{+}	A_g	A
A_{2u}^{+}	B_{1u}	B_1
A_{1u}^{-}	A_u	A
A_{2g}^{-}	B_{1g}	B_1
B_{1g}^{+}	A_g	A
B_{2u}^{+}	B_{1u}	B_1
B_{1u}^{-}	A_u	A
B_{2g}^{-}	B_{1g}	B_1
E^{+}	$B_{2u} + B_{3g}$	$B_2 + B_3$
E^{-}	$B_{2g} + B_{3u}$	$B_2 + B_3$
E_1	$A_g + A_u$	$2A$
E_2	$B_{1g} + B_{1u}$	$2B_1$
E_g	$B_{2g} + B_{3g}$	$B_2 + B_3$
E_u	$B_{2u} + B_{3u}$	$B_2 + B_3$

[a] The species notation for G_{16} (EM) is that of Merer and Watson (see Ref. 13).

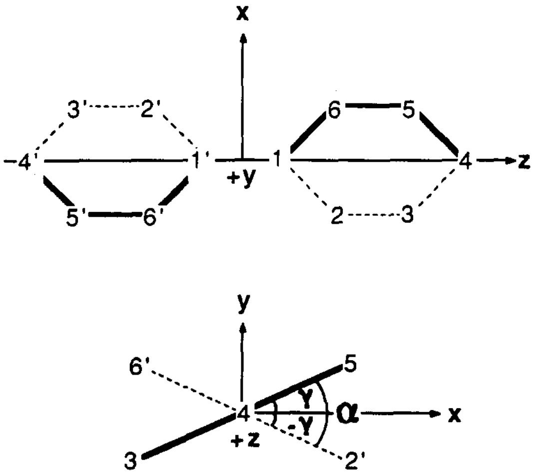

FIG. 2. Definition of molecular fixed axes and the torsional angle coordinate for BP-h_{10}. The carbons labeled 4, 1, 1′, 4′ lie on the z axis. The x, y axes vary smoothly with the torsional angle and always bisect the torsional angle. Because of the double valuedness of the torsional coordinate, the torsional angle coordinate is not the dihedral angle α but half that angle γ.

these axes with a right-hand convention.[8(d)] For some conformers, the x axis is oriented to bisect the larger torsional angle consistent with the original axis definition but contrary to Mulliken's conventional notation for rigid molecules.[11] This definition dictates that the torsional angle is $\alpha/2 = \gamma$ (defined, as usual, as increasing in the counterclockwise direction away from the x axis, observed along $+z$). The axis system and the coordinate γ are depicted in Fig. 2. With this axis system, the symmetry species for the dipole moment in G_{16} (EM) are B_{2u}^{+} (μ_z) and E_u (μ_x, μ_y).

2. Electronic state

In order to obtain the appropriate symmetry species for the electronic states of BP in G_{16} (EM) the approximate Hückel method usually used for π electron systems in rigid molecules is employed.[12] Since we must employ molecular symmetry groups, the procedure is somewhat modified.

First, label each carbon nucleus and $2p(\pi)$-electron orbital on each carbon. The $2p(\pi)$-electron orbitals are considered to be the elements of the π-system basis set for the transformation operators. Second, the elements of the symmetry group are applied to the BP molecule in the following manner: the permutation elements affect only the nuclei while the inversion elements affect the nuclei, their displacements, and the electron coordinates.[8(d)] Third, superimpose each new transformed molecular configuration on the original one. The reducible character of each element is then obtained by counting the $2p(\pi)$ orbitals whose positions are unchanged by the transformation. Fourth, reduce the reducible character set in terms of the irreducible character set and the representations of the molecular orbitals for BP are determined. Fifth, the wave functions for each molecular orbital (LCAO-MO) can be obtained, by the use of G_{16} (EM) projection operators, in terms of $2p(\pi)$-electron orbitals. The approximate energy levels can then be calculated for these MOs of specific G_{16} (EM) symmetry. The π-electrons are then placed in these orbitals and the symmetry species of the ground and various excited states are obtained in the usual manner. The ground state is found to have A_{1g}^{+} symmetry and the first excited state is found to have B_{2u}^{+} symmetry.

TABLE II. The symmetry species of the wave functions of free internal rotation in G_{16} (EM).

Symmetry species	Free internal rotation functions[a]
A_{1g}^{+}	0, + 4, + 8, ...
A_{1u}^{-}	− 2, − 6, − 10, ...
B_{1g}^{+}	+ 2, + 6, + 10, ...
B_{1u}^{-}	− 4, − 8, − 12, ...
E_1	± 1, ± 2, ± 5, ...

[a] $\phi_0 = (1/\sqrt{2\pi})$, $\phi_{+m} = (1/\sqrt{\pi})\cos m\alpha$, $\phi_{-m} = (1/\sqrt{\pi})\sin m\alpha$.

3. Torsional motion

The symmetry species of the torsional modes can be found from the one-dimensional free rotor modes of the two ring system, as classified in the G_{16} (EM) group, because the torsional modes can be written as linear combinations of the free rotor wave functions.[13] The free rotor wave function and their G_{16} (EM) symmetry species are listed in Table II.

A barrier to internal rotation in BP transforms free rotor motion into torsional motion.[14] The symmetry species of the torsional mode in the rigid conformations for BP are A in D_2 (S_0) and A_u in D_{2h} (S_1). From the correlation table (Table I) we find that A of D_2 correlates to A_{1g}^{+}, B_{1g}^{+}, E_1, A_u^{-}, and B_{1u}^{-} in G_{16} (EM). The free-rotor basis set spans this set of G_{16} (EM) irreducible representations. Therefore, one can expect (see Tables I and II) that the first eight energy levels of the free rotor converge to the first energy level of the torsional motion (fundamental) in the ground state of BP, and the next eight free-rotor levels converge to the second level (first overtone) of the D_2 torsional mode, etc. A parallel argument suggests that for the rigid planar D_{2h} excited state of BP four free-rotor levels correlate to each of the torsional motion symmetry states A_g and A_u: namely, A_{1g}^{+}, E_1, B_{1g}^{+} correlate to A_g and A_{1u}^{-}, E_1, B_{1u}^{-} correlate to A_u. The energy level correlation between the different limiting groups is depicted in Fig. 3. The calculational demonstration of this correlation is presented in the next section.

The G_{16} (EM) symmetry representations of the other normal modes of BP can be determined by considering the effect of the symmetry operations discussed above on the detailed displacement patterns of each mode.

C. Selection rules

Since the electronic and vibration eigenstates of BP are functions of the torsional angular coordinate γ, the vibronic transition moment must be written as follows[8(d)]:

$$\langle \psi'_{\rm tor} | \langle \psi'_e | \mu | \psi''_e \rangle \langle \psi'_{\rm vib} | \psi''_{\rm vib} \rangle | \psi''_{\rm tor} \rangle. \qquad (1)$$

The symbols in this expression have their usual meanings. The above matrix element must not be zero if a particular transition between ground and excited BP states is to be al-

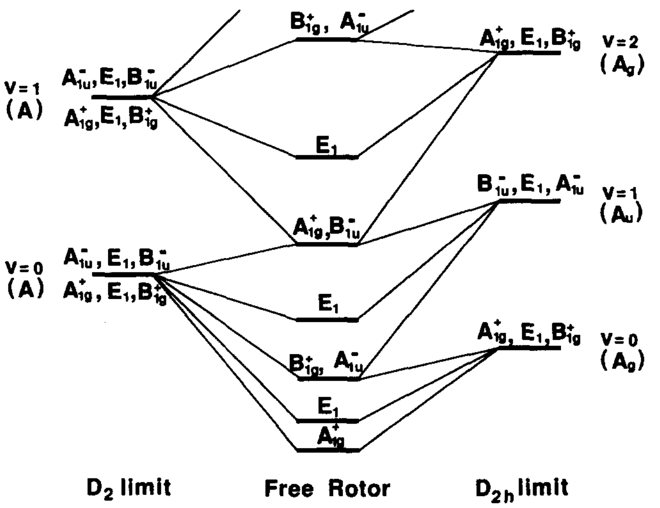

FIG. 3. The correlations of the torsional energy levels in the D_2 (S_0) and D_{2h} (S_1) limits with the free internal rotation energy levels [G_{16} (EM)] for BP-h_{10}. The v indicates the vibrational quantum number at each limit and the symmetry species in parentheses are the symmetry representations for each level in each limiting case.

lowed and thus the direct product of the symmetry species [in G_{16} (EM)] of all functions in Eq. (1) must contain the totally symmetric irreducible representation of G_{16} (EM), A^+_{1g}.

Both the 0^0_0 and any torsional level transitions are allowed under these considerations. The selection rules for other vibrational modes are that A^+_{1g}, B^+_{1g}, A^-_{1u}, B^-_{1u}, E_1, E_g, E_u, E^+, and E^- species can be observed in the spectrum. Modes which transform as irreducible representations A^+_{2u}, A^-_{2g}, B^+_{2u}, B^-_{2g}, and E_2 of G_{16} (EM) cannot be observed as fundamentals in the spectrum of BP: these species correlate to the B_{1g} and B_{1u} irreducible representations of the D_{2h} point group.

IV. CALCULATIONS OF ENERGY LEVELS AND FRANCK–CONDON FACTORS

A torsional motion is considered to be a hindered internal rotation (of the rings with respect to one another about the z molecule fixed axis) dependent only on the ring dihedral angle α ($=2\gamma$) and governed only by the potential term $V(\alpha)$. The free rotor Hamiltonian thus becomes

$$H = -B\frac{\partial^2}{\partial\gamma^2} + V(2\gamma) \tag{2}$$

in which B is the rotational constant of the rotor ($=h/8\pi^2 cI$) and I is the reduced moment of inertia about the rotation axis.[15] The general form of the potential energy term for the torsional motion is represented by a cosine Fourier series

$$V(2\gamma) = \frac{1}{2}\sum_n V_n(1-\cos 2n\gamma). \tag{3}$$

Using the wave functions of the free rotor as a basis set, the eigenfunctions for torsional motion can be expressed as

$$\psi_i(\gamma) = \sum_m C_{mi}\phi_m(\gamma), \quad m = 0, \pm 1, \pm 2, ... \tag{4}$$

in which ϕ_m is a free rotor eigenfunction with the mth free rotor quantum number and C_{mi} are the coefficients of ϕ_m in $\psi_i(\gamma)$. The ϕ_m specific to the BP coordinate system are

$$\begin{aligned} \phi_m &= \frac{1}{\sqrt{\pi}}\cos m\gamma, \quad m = 1, 2, 3, ..., \\ \phi_m &= \frac{1}{\sqrt{2\pi}}, \quad m = 0, \\ \phi_m &= \frac{1}{\sqrt{\pi}}\sin m\gamma, \quad m = -1, -2, -3, \ldots . \end{aligned} \tag{5}$$

The eigenvalues and vectors are found for the torsional motion by solving the secular determinant

$$\langle \psi_i | H - E_i | \psi_i \rangle = 0. \tag{6}$$

The nonzero matrix elements of this equation are given in Table III. Note that ψ depends on $\gamma = \alpha/2$ and $V = V(2\gamma)$. This calculation demonstrates that each torsional level of the ground electronic state (D_2 symmetry) is eightfold degenerate and each torsional level of the excited electronic state (D_{2h} symmetry) is fourfold degenerate with regard to the free-rotor G_{16} (EM) symmetry energy levels.

The calculated energy levels are fit to the observed ground and excited state torsional energy levels, as discussed below, to obtain values for the potential energy parameters. Because both accurate eigenvalues and eigenvectors (for Franck–Condon factor determination) are required from this calculation and the resulting determinant is so highly degenerate, the full determinant must be prediagonalized according to symmetry blocks before a numerical eigenvector/eigenvalue routine is employed. The individual symmetry blocks are then numerically diagonalized with the standard diagonalization routines.

The relative intensity distribution of the transitions involving overtones of the torsional motion built on the 0^0_0 in the one-color TOFMS spectrum of BP can provide information on the change in dihedral angle between the equilibrium geometry of the ground state and that of the excited state. The torsional eigenvectors can be written for the ground and excited states as $\psi''_i(\gamma)$ and $\psi'_i(\gamma+\theta)$, respectively, in which θ is the difference in the inter-ring dihedral angle between the ground state and excited state equilibrium configurations. The Franck–Condon factors for a transition between the zero-point level of the ground state and torsional levels (j) of the excited state can be expressed as[16]

$$\begin{aligned} &\langle \psi'_j(\gamma+\theta) | \psi''_0(\gamma) \rangle \\ &\quad = \left\langle \sum_{m'} C^e_{m'j}\phi_{m'}(\gamma+\theta) \,\middle|\, \sum_{m''} C^g_{m''0}\phi_{m''}(\gamma) \right\rangle \\ &\quad = \sum C^e_{mj} C^g_{mo}\cos(m\theta), \quad m = 0, \pm 1, \pm 2, \ldots . \end{aligned} \tag{7}$$

This expression is complicated by the fact that the ground and excited state energy levels appear so highly degenerate in the group of the basis set. Transitions between G_{16} (EM) states of the same symmetry are allowed and thus the transition intensity is written

Intensity (odd overtones)

TABLE III. Matrix elements associated with the Hamiltonian operator: $H = -B\frac{d^2}{d^2\gamma} + \frac{1}{2}\sum V_n(1-\cos 2n\gamma)$.

m: negative integer	m: 0 and positive integer
$\langle\phi_{m'}\vert\frac{d^2\phi}{d\gamma^2}\vert\phi_m\rangle = -m^2\ (m'=m)$	$\langle\phi_{m'}\vert\frac{d^2\phi}{d\gamma^2}\vert\phi_m\rangle = -m^2\ (m'=m)$
$\langle\phi_{m'}\vert\frac{d^2\phi}{d\gamma^2}\vert\phi_m\rangle = 0\ (m'\neq m)$	$\langle\phi_{m'}\vert\frac{d^2\phi}{d\gamma}\vert\phi_m\rangle = 0\ (m'\neq m)$
$\langle\phi_{m'}\vert V_n\vert\phi_m\rangle = V_n\ (m'=m)$	$\langle\phi_{m'}\vert V_n\vert\phi_m\rangle = V_n\ (m'=m)$
$\langle\phi_{m'}\vert V_n\vert\phi_m\rangle = 0\ (m'\neq m)$	$\langle\phi_{m'}\vert V_n\vert\phi_m\rangle = 0\ (m'\neq m)$
$\langle\phi_{m'}\vert\cos 2n\gamma\vert\phi_m\rangle = \frac{1}{2}\ (\vert m'\vert - \vert m\vert = 2n)$	$\langle\phi_0\vert\cos 2n\gamma\vert\phi_m\rangle$ $= \langle\phi_{m'}\vert\cos 2n\gamma\vert\phi_0\rangle = \frac{1}{\sqrt{2}}\ (m=2n)$
$\langle\phi_{m'}\vert\cos 2n\gamma\vert\phi_m\rangle = -\frac{1}{2}\ (\vert m'\vert + \vert m\vert = 2n)$	$\langle\phi_{m'}\vert\cos 2n\gamma\vert\phi_m\rangle = \frac{1}{2}\ (\vert m' \pm m\vert = 2n)$
$\langle\phi_{m'}\vert\cos 2n\gamma\vert\phi_m\rangle = 0\ (\vert m'\vert \pm \vert m\vert \neq 2n)$	$\langle\phi_{m'}\vert\cos 2n\gamma\vert\phi_m\rangle = 0\ (\vert m' \pm m\vert \neq 2n)$

$$\propto |\mathrm{FC}\,(A^{+}_{1g}\leftarrow A^{+}_{1g})|^2 + |\mathrm{FC}\,(E_1\leftarrow E_1)|^2 + |\mathrm{FC}\,(B^{+}_{1g}\leftarrow B^{+}_{1g})|^2 + |\mathrm{FC}\,(E_1\leftarrow E_1)|^2,$$

Intensity (even overtones)

$$\propto |\mathrm{FC}\,(A^{-}_{1u}\leftarrow A^{-}_{1u})|^2 + |\mathrm{FC}\,(E_1\leftarrow E_1)|^2 + |\mathrm{FC}\,(B^{-}_{1u}\leftarrow B^{-}_{1u})|^2 + |\mathrm{FC}\,(E_1\leftarrow E_1)|^2. \tag{8}$$

The different symmetry G_{16} (EM) free rotor eigenstates comprising the D_2 and D_{2h} rigid molecule torsional levels do not mix and are thereby in a sense "accidentally" degenerate: the expressions in Eq. (8) are thus properly "incoherent" sums. The E_1 states are truly degenerate, however, and their sums must be obtained "coherently"; i.e.,

$$|\mathrm{FC}\,(E_1\leftarrow E_1)|^2 = (|\mathrm{FC}\,(E_{1a}\leftarrow E_{1a})| + |\mathrm{FC}\,(E_{1b}\leftarrow E_{1b})|)^2. \tag{9}$$

The displacement angle θ is determined by a best fit to the experimental observations: if the equilibrium ground state confirmation is known, the equilibrium excited state conformation can be determined.

V. RESULTS AND INTERPRETATIONS

The one-color TOFMS of the $S_1 \leftarrow S_0$ transition of BP is presented in Fig. 4 and the features are assigned in Table IV. The intensity of the 0_0^0 transition is quite small for this system and a very long progression in the torsional mode can readily be identified. The general form of this spectrum is expected based on the assumed large conformational change undergone by BP upon S_0 to S_1 excitation. Consequently, the assignment of the origin is not immediately obvious. Many theoretical[17] and experimental (solutions,[18] crystals[19]) studies have served for estimates of the origin position in the spectrum but these are not accurate enough to assist in the gas phase determination of the 0_0^0 band.

A. 0_0^0 transition

The peak at 35 258.0 cm^{-1}, the lowest energy cold feature in the spectrum, is assigned to be the $S_1 \leftarrow S_0$ origin or 0_0^0 transition. This feature is shifted to the blue by approximately 2100 cm^{-1} from the assigned 0_0^0 in the crystal: this gas-to-crystal shift is comparable to that observed for tolane.[20] Several experimental results support this assignment. First, the general pattern of the spectrum and the detailed peak positions for BP-h_{10}, BP-h_5d_5, and BP-d_{10} are all very similar in this spectral region even including the small observed negative anharmonicity in the torsional mode (see Fig. 5 and Table V). This is good evidence in support of the origin assignment in all three samples. Second, comparison of the origin shift for substituted BPs with respect to the BP as-

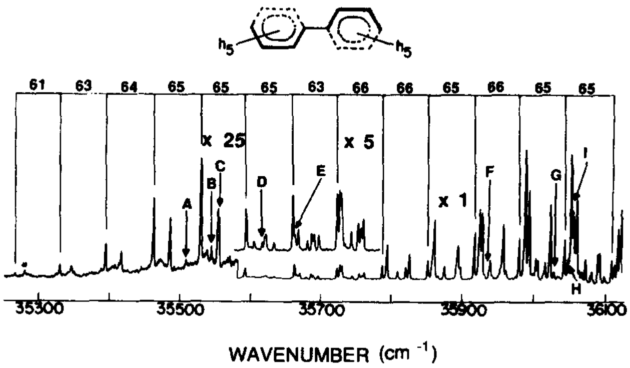

FIG. 4. One-color TOFMS of BP-h_{10} in a supersonic expansion of argon at 10 psig. The weak feature at 35 268 cm^{-1} is tentatively assigned as the $S_1 \leftarrow S_0$ origin (0_0^0) band. The torsional progression is bracketed with excited state torsional spacings shown in cm^{-1}. The peak marked by * is assigned as the sequence band of the torsional mode (T_1^1). The peaks marked with capital letters are vibrational mode fundamentals in S_1 (cf. Table IX).

TABLE IV. TOFMS spectrum and assignments for BP-h_{10} in the energy range 35 240–36 140 cm^{-1}.

ν (cm^{-1})	$\nu - \nu(0^0_0)$ (cm^{-1})	Assignment[a]
35 258.0	0	0^0_0
35 270.8	12.8	T^1_1
35 319.4	61.4	T^1_0
35 335.6	77.6	T^2_1
35 382.6	124.6	T^2_0
35 404.5	146.5	T^3_1
35 430.2	172.2	A^1_0
35 447.7	189.7	T^3_0
35 470.1	212.1	T^4_1
35 491.8	233.8	$A^1_0T^1_0$
35 512.1	254.1	T^4_0
35 527.1	269.1	B^1_0
35 536.7	278.7	T^5_1
35 538.1	280.1	C^1_0
35 553.2	295.2	$A^1_0T^2_0$
35 577.1	319.1	T^5_0
35 588.1	330.1	$B^1_0T^1_0$
35 600.4	342.4	D^1_0
35 603.2	345.2	T^6_0
35 604.5	346.5	$C^1_0T^1_0$
35 615.8	357.8	$A^1_0T^3_0$
35 642.2	384.2	T^6_0
35 645.6	387.6	E^1_0
35 649.7	391.7	$B^1_0T^2_0$
35 663.3	405.3	$D^1_0T^1_0$
35 670.2	412.2	T^7_1
35 673.0	415.0	$C^1_0T^2_0$
35 680.5	422.5	$A^1_0T^4_0$
35 705.4	447.4	T^7_0
35 709.5	451.5	$E^1_0T^1_0$
35 711.9	453.9	$B^1_0T^3_0$
35 728.4	470.4	$D^1_0T^2_0$
35 735.7	477.7	T^2_1
35 741.9	483.9	$C^1_0T^3_0$
35 745.3	487.3	$A^1_0T^5_0$
35 771.5	513.5	T^8_0
35 778.0	520.0	$E^1_0T^2_0,{}^1_0T^4_0$(d)
35 793.5	535.5	$D^1_0T^3_0$
35 805.3	547.3	T^9_1
35 809.8	552.8	$C^1_0T^4_0,A^1_0T^6_0$(d)
35 835.9	577.9	T^9_0
35 842.1	584.1	$E^1_0T^3_0$
35 844.9	586.9	$B^1_0T^5_0$
35 858.9	600.9	$D^1_0T^4_0$
35 875.7	617.7	T^{10}_0
35 878.5	620.5	$C^1_0T^5_0,A^1_0T^7_0$(d)
35 900.8	642.8	T^{10}_0
35 908.5	650.5	$E^1_0T^4_0$
35 912.0	654.0	$B^1_0T^6_0$
35 923.9	665.9	F^1_0
35 925.3	667.3	$D^1_0T^5_0$
35 940.6	682.6	T^{11}_1
35 944.1	686.1	$C^1_0T^6_0,A^1_0T^8_0$(d)
35 966.5	708.5	T^{11}_0
35 974.6	716.6	$E^1_0T^5_0$
35 979.7	721.7	$B^1_0T^7_0$
35 990.2	732.2	$F^1_0T^1_0$
35 993.0	735.0	$D^1_0T^6_0$
36 003.6	745.6	T^{12}_1
36 011.2	753.2	$C^1_0T^9_0,A^1_0T^9_0$(d)
36 017.5	759.5	G^1_0
36 031.3	773.3	T^{12}_0
36 037.0	779.0	H^1_0
36 040.6	782.6	$E^1_0T^6_0$
36 043.5	785.5	I^1_0
36 048.5	790.5	$B^1_0T^8_0$
36 056.4	798.4	$D^1_0T^7_0$
36 061.4	803.4	$F^1_0T^2_0$
36 070.0	812.0	T^{13}_1
36 078.6	820.6	$C^1_0T^8_0$
36 081.5	823.5	$A^1_0T^{10}_0$
36 087.9	829.9	$G^1_0T^1_0$

[a] A through I are the notations for the observed S_1 modes of BP-h_{10}. T is the notation for the torsional modes in S_1 of BP-h_{10}.

signed origin and the substituted toluenes with respect to the intense toluene origin presents very similar trends (see Table VI) for both series. This again is corroborating evidence that favors the present 0^0_0 assignment of the spectrum. We are thus reasonably confident that the $S_1 \leftarrow S_0$ 0^0_0 transition for BP-h_{10} lies at 35 258.0 cm^{-1}.

B. Torsional modes

A long harmonic progression is built on the origin at 35 258.0 cm^{-1}, the spacing of which is ~65 cm^{-1} for BP-h_{10}

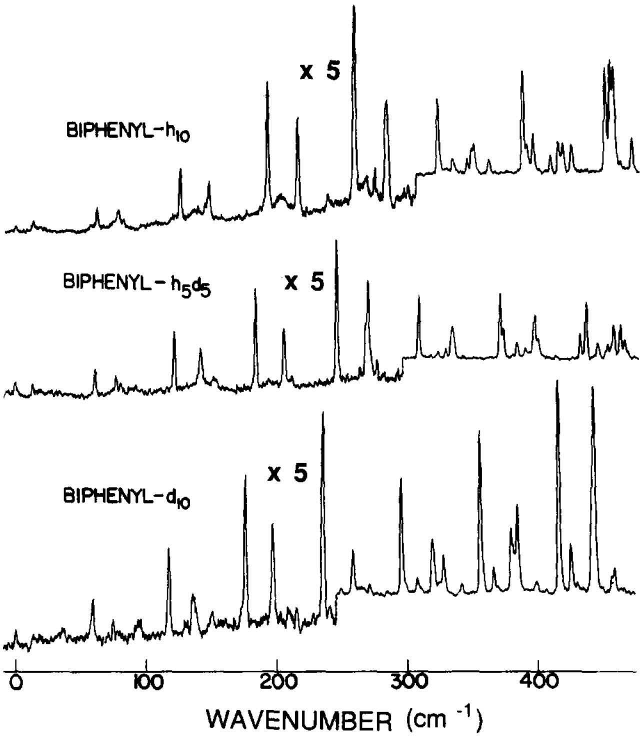

FIG. 5. The TOFMS of BP-h_{10}, BP-h_5d_5, and BP-d_{10} around 0^0_0 region of each species. The S_1 origins of BP-h_5d_5 and BP-d_{10} are at 35 367.4 and 35 469.6 cm^{-1}, respectively. The pattern of the spectra of these three isotopic species is nearly identical. The spectra show the isotope effect on the spacings of the torsional vibration.

TABLE V. The observed torsional spacings for S_1 of BP-h_{10}, BP-h_5d_5, BP-d_{10}.

Assignment\Samples	BP-h_{10}	BP-h_5d_5	BP-d_{10}
T_0^1	61.4	60.4	58.0
T_0^2	63.2	60.7	58.6
T_0^3	64.1	61.9	58.7
T_0^4	65.4	62.0	60.2
T_0^5	65.0	62.8	60.7
T_0^6	65.1	63.1	61.1
T_0^7	63.2	65.7	60.8
T_0^8	66.1	63.7	60.7
T_0^9	66.4	64.9	60.6
T_0^{10}	64.9	65.0	60.5
T_0^{11}	65.7	···	61.2
T_0^{12}	64.8	···	60.8
T_0^{13}	65.4	···	62.1

(see Table V and Figs. 4 and 5). The peak intensity in this progression increases to the eleventh member (T_0^{11}) and then begins to decrease. Figure 5 and Table V show the isotope effect on this progression. Chemical derivatives of BP at the 4-position or the 4,4′-positions show little or no substitution effect for this torsional progression while derivatives at other positions show considerable changes in the progression and its interval (see Fig. 6). The frequencies for the torsional motions of all biphenyls studied are collected in Table VII. We can conclude from these data that the main progression observed is that of the z axis torsional mode.

The best fit potential parameters are obtained by matching the observed and calculated torsional spacings. V_2, V_4, V_6 potential parameters are required for the excited state surface and V_2 and V_4 parameters are required for the ground state surface. The results of such calculations are found in Table VIII. The eigenvectors obtained for this energy level set are used to determine Franck–Condon intensity factors and the displacement angle θ. θ is found to be 44°.

C. Sequence bands

Additional transitions appear in the spectrum of BP that are not members of the 0_0^0 torsional mode progression (T_0^n). In particular, a feature can be observed at 13 cm^{-1} to the blue of the 0_0^0 transition (see Fig. 4): this feature serves as an origin for another progression in the torsional mode. The feature and the progression built on it also appear in the BP-h_5d_5 and BP-d_{10} spectra. This 13 cm^{-1} feature can be assigned as (1) a low frequency fundamental, (2) a BP–Ar cluster fragmentation peak, (3) an exciton state, and (4) a sequence band. The first two options can be dismissed quickly. The 13 cm^{-1} feature is too low in energy for any fundamental considering that the lowest (out-of-plane) mode in S_0 is 77 cm^{-1} and that the molecule becomes more rigid in the excited state. This feature and its progression are present

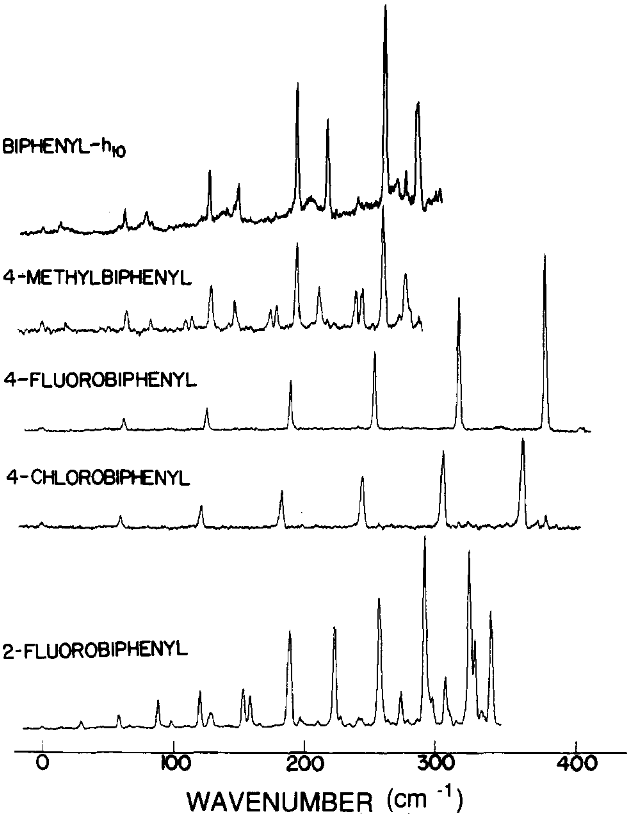

FIG. 6. The TOFMS of BP-h_{10}, 4-CH_3–BP, 4-F–BP, 4-Cl–BP, and 2-F–BP around their 0_0^0 regions. The S_1 origins of the species are as follows: 4-CH_3–BP (34 649.2 cm^{-1}), 4-F–BP (34 626.2 cm^{-1}), 4-Cl–BP (34 497.7 cm^{-1}), and 2-F–BP (35 435.9 cm^{-1}). The torsional spacings are nearly the same for the derivatives substituted at position 4. For 2-F–BP, the torsional spacings are significantly reduced.

TABLE VI. The substituent effect on the position of the S_1 origin in biphenyl derivatives.

Substituent	Biphenyl (35 258.0 cm^{-1})[a]	Toluene (37 477.4 cm^{-1})[a]
4-CH_3	− 609[b]	− 744
4-F	− 632	− 617
2-F	+ 235	+ 84
4-Cl	− 760	c

[a] The figures in parentheses are the origin of each species.

[b] The negative sign indicates red shift and the positive sign indicates blue shift from the S_1 origin of its nonsubstituted species.

[c] No data are available for this species.

TABLE VII. The energy of the torsional motion in the S_1 state for biphenyl and its derivatives.

Samples	Energy (cm^{-1})
BP-h_{10}	65
BP-h_5d_5	63
BP-d_{10}	60
4-CH_3–BP	66
4-CD_3–BP	66
4-4′-$(CH_3)_2$–BP	70
4-F–BP	64
4-4′-$(F)_2$–BP	70
4-Cl–BP	60
2-F–BP	35

TABLE VIII. Experimental and calculated S_1 torsional energy levels of BP-h_{10}.

Assignment	$\Delta\nu_{\rm exptl}$ (cm^{-1})[a]	$\Delta\nu_{\rm calcd}$ (cm^{-1})[b]
T^1	61.4	61.7
T^2	124.6	124.4
T^3	189.7	188.0
T^4	254.1	252.5
T^5	319.1	317.6
T^6	384.2	383.3
T^7	447.4	449.3
T^8	513.5	515.4
T^9	577.9	581.5
T^{10}	642.8	647.3
T^{11}	708.5	712.7
T^{12}	773.3	777.5
T^{13}	840.7	841.2

[a] Measured from the vibrationless level of the S_1 state, i.e., the zero-point level of the torsional potential.

[b] In the calculation, the following parameters are used: $B = 0.387$ cm^{-1} (the reduced rotational constant), $V_2 = 1195.0$ cm^{-1}, $V_4 = -190.0$ cm^{-1}, $V_6 = 18$ cm^{-1}.

as BP-h_{10}, BP-d_{10}, and BP-h_5d_5 are expanded in He and N_2. Choice three above would suggest that the interaction between the rings is quite small (~ 13 cm^{-1}): thus this exchange effect should be removed in the mixed isotope BP-h_5d_5 which is certainly not the case. We discuss the exciton interaction between the ring more completely below.

Finally we are left with the conclusion that the 13 cm^{-1} feature is a sequence band. We suggest that this is a sequence band of the torsional motion with an S_0 fundamental value of ~ 50 cm^{-1} and an S_1 fundamental value of ~ 65 cm^{-1}.

D. The remaining features

In addition to the main torsional progressions built on the 0_0^0 and 13 cm^{-1} hot band transitions, other vibrational modes are found in the spectra of BP and its derivatives. A number of other assignments can be tentatively suggested based on the ground state fundamentals,[21] selection rules, and spectra of various BP derivatives. Table IX contains a summary of these assignments. Since in the D_{2h} symmetry excited state the molecule is quite rigid and planar, a number of the out-of-plane bending and stretching motions will increase in energy as the molecule undergoes the $S_1 \leftarrow S_0$ transition.[22]

TABLE IX. The suggested correlation of the fundamentals in S_1 with those in S_0.

Fundamentals (cm^{-1}) in S_1	Fundamentals (cm^{-1}) in S_0	Mode
172.2 (*A*)[a]	116 (B_{2u})[b]	in-plane bend
269.1 (*B*)	260 (B_{2g})	···
280.1 (*C*)	2×91 (B_{1u})	out-of-plane bend
342.4 (*D*)	?	?
387.6 (*E*)	315 (A_g)	stretch
667.3 (*F*)	609 (B_{3u})	···
795.5 (*G*)	?	?
779.0 (*H*)	2×315 (A_g)	stretch (overtone)

[a] The characters in the parentheses indicate the assignments in Table IV.

[b] The symmetry species in D_{2h} the planar geometry of biphenyl. Data from Ref. 21.

E. Inter-ring exciton interaction

The magnitude of the exciton interaction in BP must be at least greater than 200 cm^{-1} because E(BP-h_{10}) $-$ E(BP-d_{10}) ≈ 200 cm^{-1} and BP-h_5d_5 has the same spectral structures does BP-h_{10} and BP-d_{10}. One can get some qualitative appreciation for the size of this interaction by studying asymmetrical derivatives of BP, such as F–, Cl–, CH_3–BP, for which the ring resonance is removed by more than 600 cm^{-1}. While the absolute energies of the 4-CH_3–BP and BP spectra are quite different, the qualitative features are quite similar and the 0_0^0 energy shifts for the substituted molecules suggest only substituent shifts and not resonance interaction differences (see Fig. 6 and Table VI). Of course some new features appear for 4-CH_3–BP, but since they also appear for 4-$(CH_3)_2$–BP and 4-CD_3–BP their exciton origin is not substantiated (see Fig. 7). In particular, the doublet feature at ~ 115 cm^{-1} in 4-CH_3–BP appears at ~ 90 cm^{-1} in 4-CD_3–BP. Since the splitting of the feature is roughly constant and its isotope shift is $\sim 20\%$, we suggest that this feature is a sequence band. Note that in the asymmetrically monosubstituted BP systems both exciton components should be allowed and possibly observed. Different patterns arise for the spectra of 4-F–BP, 4-F_2–BP (Fig. 8), and 4-Cl–BP (Fig. 6). No hot bands are found in these systems and only the torsional mode progression is seen below 300 cm^{-1} to higher energy of the origin. The spectra of 4-F–BP and 4-F_2–BP are also very similar.

The main conclusion here is that the inter-ring exciton interaction is quite large, probably greater than 1000 cm^{-1}. More will be said about this point in the Discussion.

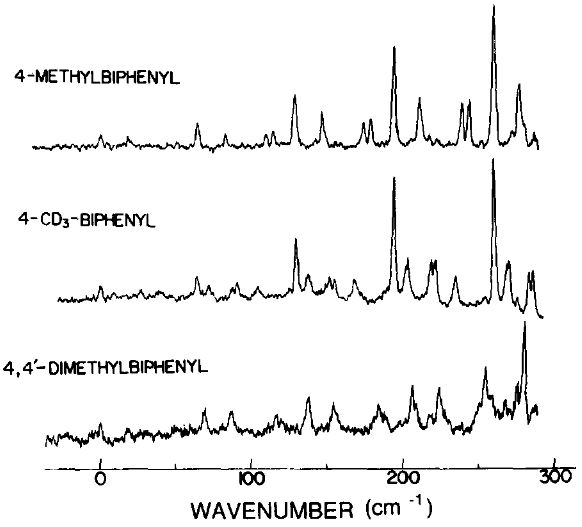

FIG. 7. The TOFMS of 4-CH_3–BP, 4-CD_3–BP, 4-4'-$(CH_3)_2$–BP around their S_1 origin regions. The S_1 origins of 4-CD_3–BP, 4-4'-$(CH_3)_2$–BP are (34 664.8 cm^{-1}) and (34 312.4 cm^{-1}), respectively. The spectra of these derivatives are quite similar to those of BP-h_{10}.

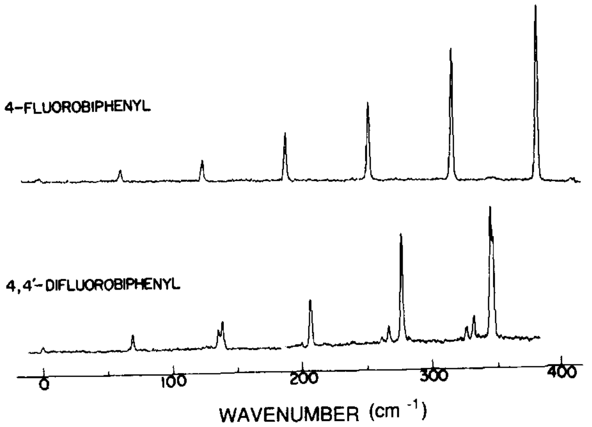

FIG. 8. The TOFMS of 4-F–BP and 4-4'-(F)$_2$–BP around their 0_0^0 regions. The S_1 origin of 4-4'-(F)$_2$–BP is (34 270.8 cm^{-1}). The spectra of the two species show similar patterns.

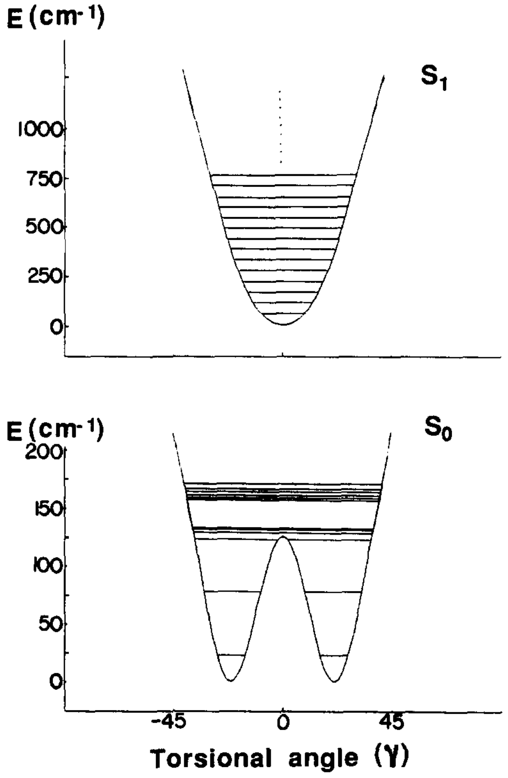

FIG. 9. Best-fit effective potentials for the torsional motion of BP-h_{10} in the excited state (top) and the ground state (bottom). In the excited state, the potential has a single minimum and in the ground state the potential has double a minimum. The potential barrier of the ground state is shallow so one can expect a large anharmonicity in the torsional levels. The potential barrier is large in the excited state and the torsional level is expected to be harmonic.

VI. DISCUSSION

In this section we discuss our three most important results: the torsion mode frequency and thus the ground and excited state potential energy surfaces for BP nonrigid internal motion; the intensity pattern (Franck–Condon factors) for the torsional mode progressions observed and thus the S_0–S_1 displacement angle θ; and the inter-ring exciton interaction.

A. Torsional mode frequency and excited state geometry

As the progression in the torsional mode increases in energy, its intensity and spacings become more difficult to identify due to spectral crowding and possible Fermi resonances with other fundamental and combination modes. This can be seen in Fig. 4 and Tables IV and VIII for BP-h_{10}. Intensity and frequency problems are the most obvious at the seventh to eighth member of the BP T_0^n progression for which this feature clearly becomes a triplet: the specific peak is difficult to identify and the intensity is confused. The proper spacings, features, and intensity pattern can nonetheless, be extracted by comparison with spectra of other isotopically and chemically substituted BPs as evidenced in Figs. 5 and 6 and Tables V and VII. Note, however, that the intensity maximum for the chemically substituted biphenyls occurs at peaks 16 to 18 of the T_0^n progression. The ground state angle and T_1 mode fundamental energy are different in the chemically substituted biphenyls from those found in biphenyl itself even though the S_1 T^1 fundamental seems quite similar.

Calculations also assist in the assignment of the maximum intensity peak in the T_0^n progression: 625 free-rotor basis functions are employed to calculate 22 torsional mode levels. Accurate energy values for this progression are obtained, by including a negative anharmonicity which is uniquely generated by a negative V_6 term.

In order to determine the torsion angle difference between the ground and excited state, good Franck–Condon overlap integrals must be obtained from accurate vibrational wave functions for the observed progression. Thus the ground state potential surface must be determined. A previous determination[23] of the ground state z torsion gives a fundamental energy of 105 cm^{-1}.[24] This is clearly too large: the ground state value must be considerably less than 65 cm^{-1} because the excited state is considerably more rigid than the ground state. Based on sequence and hot bands we have chosen a T_1 energy of ~ 50 cm^{-1} (see Table IV). Unfortunately, dispersed emission spectra could not be observed at high enough intensity to obtain a value for the ground state torsion directly. The ground state potential values are $V_2 = 50$ cm^{-1} and $V_4 = -148$ cm^{-1}. The ground and excited state surfaces are plotted in Fig. 9. With S_0 and S_1 eigenfunctions for the torsional mode, the Franck–Condon intensity pattern for the T_0^n torsional progression is calculated as presented in Eqs. (7), (8), and (9). Peak eight in the progression is always calculated to be the most intense for a wide range of S_0 potential parameters V_2 and V_4. This coincides with the observations for BP-d_{10} and BP-h_5d_5: the BP-h_{10} spectrum must be perturbed in this region by Fermi resonance and spectral congestion. The intensity patterns observed for the chemically substituted BPs are also consistent with this determination of the maximum intensity peak in the T_0^n progression. The value of the excited state displacement angle is thus $\theta = 44°$ for the isotopically substituted BPs and the two aromatic rings in BP are within experimental error coplanar in the S_1 excited state.

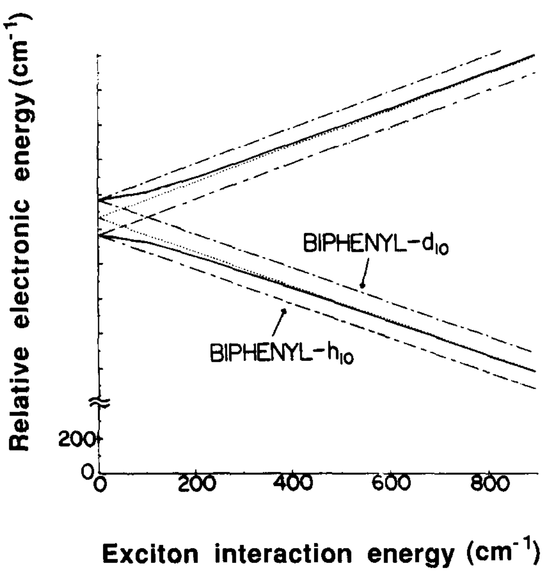

FIG. 10. The electronic energy splitting for S_1 as a function of the magnitude of the exciton interaction. The energy levels for the h_{10} and d_{10} species are marked on the figure with a dot–dash line. The solid line refers to the energy levels of BP-h_5d_5. The dotted line marks the energy center between BP-h_{10} and BP-d_{10} energies. The energy of BP-h_5d_5 coincides with the energy center between the BP-h_{10} and BP-d_{10} features for large (> 10^3 cm^{-1}) excitation interaction. This energy relation between the three BP isotopes is exactly what is observed experimentally.

B. Estimate of the inter-ring exciton interaction in S_1

The biphenyl molecule has been thought of in the past as a strongly coupled dimer of benzene.[7(b)] This approximation leads one to think of the inter-ring interaction in the biphenyl S_1 state in terms of exchange or exciton interactions.[25]

The three isotopically substituted BPs (h_{10}, d_{10}, h_5d_5) give strong evidence that this interaction is quite large as demonstrated in Fig. 10. If the exciton interaction is small (the benzene case),[25] isotopic substitution should diminish the effect of the exciton interactions on the observed h_5d_5 energy levels. Thus for exciton interactions that are comparable to the 200 cm^{-1} d_{10}/h_{10} isotopic shift, nonlinear effects on the h_5/d_5 transition energy would be observed. One would not expect to observe in this instance the 0, 100, 200 cm^{-1} h_{10}, h_5d_5, d_{10} symmetrical linear energy differences that are apparent in the spectra (see Table X). Moreover, the isotope effect observed for $h_{10}/h_5d_5/d_{10}$ is exactly that expected considering separate benzene rings in the strong coupling limit. Thus the exciton interaction must be quite large for BP, probably greater than 10^3 cm^{-1}. This conclusion is well substantiated by the asymmetrical chemically substituted BP for which both levels of the exciton structure should be observed.

TABLE X. The isotope effect on the shift of S_1 origin.

Species	$\Delta\nu_{\text{exptl}}$ (cm^{-1})	$\Delta\nu_{\text{calcd}}$ (cm^{-1})
BP-h_{10}	0	0
BP-h_5d_5	99	99
BP-d_{10}	201	198

VII. CONCLUSIONS

Cooling biphenyl and its derivatives in a supersonic expansion removes both sequence structure and hot band structure to the extent that good high resolution vibronic spectra (TOFMS) can be obtained and analyzed for this set of molecules.[26] Our work has lead to the following conclusions:

(1) The extended molecular symmetry group [G_{16} (EM)] is the appropriate group for the free biphenyl molecule. All biphenyl energy levels can be characterized by the irreducible representations of G_{16} (EM). Selection rules for contorsional, vibrational, and electronic transitions can be determined with this group.

(2) The lowest singlet excited state of BP is of B_{2u}^{+} symmetry in G_{16} (EM) and the transition from S_0 to S_1 is allowed.

(3) Torsional frequencies are identified for all BP isotopes and chemically substituted species studied.

(4) Potential parameters are determined for this torsional mode in both the S_0 and S_1 states for BP.

(5) A Franck–Condon analysis of the T_0^n torsional progression yields the change in the ring dihedral angle upon excitation. The rings are coplanar in S_1 but rotated by $\sim 44°$ with respect to each other in the ground state.

(6) Biphenyl in the S_1 state should probably not be considered as a dimer of benzene. The exciton interaction between the two "components" of biphenyl in the S_1 state is quite large; probably greater than 10^3 cm^{-1}. This large exchange interaction is of course consistent with the observed planar geometry in this state.

ACKNOWLEDGMENTS

We wish to thank J. I. Seeman and H. V. Secor of the Philip Morris USA Research Corporation for synthesizing BP-h_5d_5 and 4-CD$_3$–BP for us. We had many helpful and informative discussions with J. I. Seeman concerning this work. This work was supported in part by the ONR.

[1] (a) A. Golebiewski and A. Parczewski, Theor. Chim. Acta (Berlin) **7**, 171 (1967); (b) A. Gamba, E. Rusconi, and M. Simonetta, Tetrahedron **26**, 871 (1970); (c) M. F. M. Post, J. K. Eweg, J. Langelaar, J. D.W.VanVoorst, and G. Termaten, Chem. Phys. **14**, 165 (1976).

[2] H. T. Jonkman and D. A. Wiersma, J. Chem. Phys. **81**, 1573 (1984).

[3] (a) D. W. Werst, W. R. Gentry, and P. F. Barbara, J. Phys. Chem. **89**, 729 (1985); (b) D. W. Werst, Ann M. Brearley, W. R. Gentry, and P. F. Barbara, J. Am. Chem. Soc. **109**, 34 (1987).

[4] K. Yamasaki, K. Arita, O. Kajimoto, and K. Hara, Chem. Phys. Lett. **123**, 277 (1986).

[5] J. Murakami, M. Ito, and K. Kaya, J. Chem. Phys. **74**, 6505 (1981).

[6] A. Imamura and R. Hoffman, J. Am. Chem. Soc. **90**, 5379 (1968).

[7] (a) H. Suzuki, *Electronic Absorption Spectra and Geometry of Organic Molecules* (Academic, New York, 1967); (b) D. S. McClure, Can. J. Chem. **36**, 59 (1958).

[8] (a) H. C. Longuet-Higgins, Mol. Phys. **6**, 445 (1963); (b) J. K. Watson, Can. J. Phys. **43**, 1996 (1965); (c) J. T. Hougen, *ibid.* **42**, 1920 (1964); (d) P. R. Bunker, *Molecular Symmetry and Spectroscopy* (Academic, New York, 1979).

[9] E. R. Bernstein, K. Law, and M. Schauer, J. Chem. Phys. **80**, 207 (1984).

[10] H. Suzuki, Bull. Chem. Soc. Jpn. **32**, 1340 (1959).

[11] R. S. Mulliken, J. Chem. Phys. **23**, 1997 (1955).

[12] F. A. Cotton, *Chemical Application of Group Theory* (Wiley, New York, 1963).

[13] A. J. Merer and J. K. Watson, J. Mol. Spectrosc. **47**, 499 (1973).

[14] D. G. Lister, J. N. MacDonald, and N. L. Owen, *Internal Rotation and Inversion* (Academic, New York, 1978).

[15] K. S. Pitzer, J. Chem. Phys. **14**, 239 (1946).

[16] K. Okuyama, N. Mikami, and M. Ito, J. Phys. Chem. **89**, 5617 (1985).

[17] For example, see Y. Gondo, J. Chem. Phys. **41**, 3928 (1964), and references in this paper.

[18] E. C. Lim and Y. H. Li, J. Chem. Phys. **52**, 6416 (1970), and references in this paper.

[19] (a) R. Coffman and D. S. McClure, Can. J. Chem. **36**, 48 (1958); (b) R. M. Hochstrasser, R. D. McAlpine, and J. D. Whiteman, J. Chem. Phys. **58**, 5078 (1973).

[20] K. Okuyama, T. Hasegawa, M. Ito, and N. Mikami, J. Phys. Chem. **88**, 1711 (1984).

[21] (a) G. Zerbi and S. Sandroni, Spectrochim. Acta Part A **24**, 483 (1968); (b) **24**, 511 (1968). (c) R. M. Barrett and D. Steele, J. Mol. Struct. **11**, 105 (1972), and Refs. 9(b) and 9(c).

[22] H. H. Jaffe and M. Orchin, *Theory and Applications of Ultraviolet Spectroscopy* (Wiley, New York, 1966), Chap. 15.

[23] A. Almenningen, O. Bastiansen, L. Fernholt, B. N. Cyrin, S. J. Cyvin, and S. Samdal, J. Mol. Struct. **128**, 59 (1985).

[24] Reference 23 reports potential parameters for the torsional motion in the ground state as $V_2 = 41.7$ cm^{-1} and $V_4 = -516.5$. With these values, the first energy level of the torsional motion is calculated to be 105 cm^{-1} and the progression maximum peak is predicted to be at the eighth band. These results, however, do not coincide with the observations. First, the energy of T_1 should be smaller than the energy of T^1. Second, the relative intensitites in the progression must be correct. For example, the intensity rates for $0^0_0 : T^1_0$ is roughly 1:50 from observation and our calculation but 1:200 for the potentials given above.

[25] (a) E. R. Bernstein, S. D. Colson, R. Kopelman, and G. W. Robinson, J. Chem. Phys. **48**, 5596 (1968); (b) S. D. Colson, *ibid.* **48**, 3324 (1968); (c) S. D. Colson and T. L. Netzel, Chem. Phys. Lett. **16**, 555 (1972); (d) J. M. Van Pruyssen and S. D. Colson, Chem. Phys. **6**, 382 (1974).

[26] The data for the S_1 origins and the fundamentals of the derivatives of biphenyl in the excited state will be reported in the Ph.D. dissertation of H. S. Im, Colorado State University, 1989.